

See discussions, stats, and author profiles for this publication at: <https://www.researchgate.net/publication/341525806>

# Towards Smart Cities: Crowdsensing-based Monitoring of Transportation Infrastructure using Moving Vehicles

Article in *Journal of Civil Structural Health Monitoring* · June 2020

DOI: 10.1007/s13349-020-00411-6

---

CITATIONS

0

---

READS

206

1 Towards Smart Cities: Crowdsensing-based Monitoring of Transportation Infrastructure using Moving  
2 Vehicles

3 <sup>1</sup>Qipei Mei, <sup>2</sup>Mustafa Gül, <sup>1</sup>Nima Shirzad-Ghaheroudkhani

4 <sup>1</sup> Ph.D. Student

5 <sup>2</sup>Associate Professor (Corresponding Author: [mustafa.gul@ualberta.ca](mailto:mustafa.gul@ualberta.ca))

6 Department of Civil and Environmental Engineering, University of Alberta

7 Edmonton, Alberta, T6G 2W2, Canada

8 **Abstract:** This paper presents a novel framework for transportation infrastructure monitoring using sensors  
9 in crowdsourced moving vehicles. Vehicles equipped with various kinds of sensors have the potential to be  
10 the perfect tools for assessing the overall health condition of transportation infrastructure at the city level.  
11 Three applications of crowdsensing-based techniques are introduced in this paper to evaluate the  
12 framework. First, a methodology using the vibration data collected from a large number of smartphones in  
13 moving vehicles for bridge damage detection is presented. Lab experiments are conducted to verify the  
14 method. Second, a lab experiment investigating the feasibility of gyroscope in smartphones for road  
15 deformation measurement is described. Third, a sport camera is used to assess road surface condition.  
16 These three applications demonstrate the potential of crowdsensing-based techniques to accomplish low-  
17 cost and efficient transportation infrastructure monitoring.

18 **Keywords: Crowdsensing; Transportation Infrastructure Monitoring; Moving Vehicles**

19 **1. Introduction**

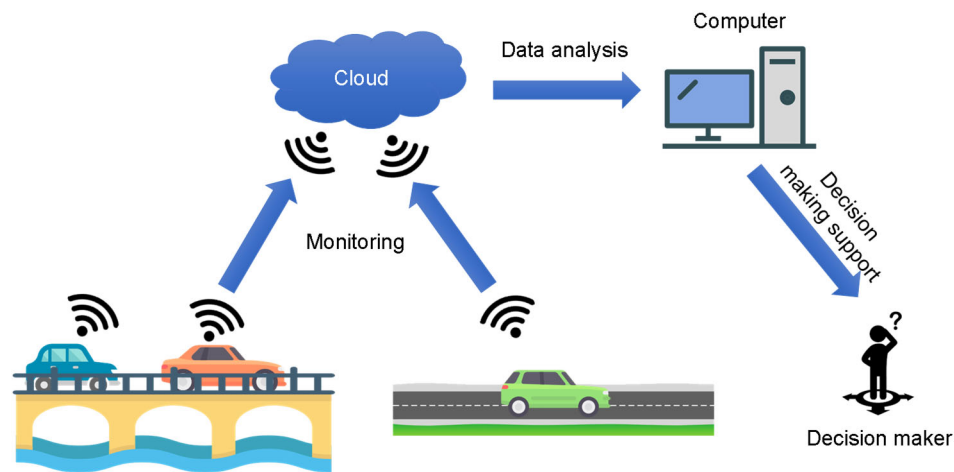
20 Improving the efficiency and sustainability of transportation infrastructure systems is a major  
21 undertaking in the future development of smart cities [1-3]. In this context, advanced sensing and data  
22 analytics offer unique capabilities for improving various components of transportation infrastructure systems.  
23 Currently, transportation infrastructure systems in developed countries, as key components of smart cities,  
24 are mostly outdated and are vulnerable to various risks [4,5]. As these transportation infrastructure systems  
25 age, there is an increasing demand for cost effective and efficient tools to monitor and manage the systems  
26 due to the limited budget of municipal jurisdictions.

27 Currently, there are two common methods used to monitor existing transportation infrastructure systems.  
28 The first method involves pre-installing sensors on the infrastructure to continuously collect and analyze data.  
29 The second method involves occasionally dispatching engineers or technicians to the site to record the  
30 measurements and bring them back for analysis. In spite of the rapid development of these monitoring  
31 techniques, there are still challenges in terms of scalability, i.e., applying these techniques to all of the existing  
32 transportation infrastructure systems. For the first method described above, a large number of sensors must  
33 be pre-installed on the infrastructure components. The cost for sensors and the cost of the labor to install them  
34 are high, and providing stable power supply systems for this type of health monitoring system remains an  
35 unresolved problem. For the second method, the inspection intervals are usually long due to the high costs of  
36 labor and inspection equipment.

37 To overcome the abovementioned issues, researchers have proposed using vehicles that are equipped  
 38 with various kinds of sensors to monitor the transportation infrastructure systems with the involvement of  
 39 citizens to increase efficiency and reduce the cost to municipal departments [6,7]. Owing to the high mobility  
 40 of vehicles, they can efficiently monitor the health condition of a population of the existing infrastructure.  
 41 Figure 1 includes a list of widely used sensors in vehicles. The monitoring strategy that uses crowdsourced  
 42 sensors in vehicles is presented in Figure 2. The sensors in vehicles can collect data while the vehicle is  
 43 traveling along a road or over a bridge. Then, the data are transmitted to remote servers for further processing  
 44 and decision making. In employing this strategy, there is no need to install sensors locally, and monitoring  
 45 the condition of the infrastructure can be accomplished efficiently with the involvement of a large number of  
 46 vehicles.



47  
 48 Figure 1 – Sensors that can be installed in vehicles (modified from [8])  
 49



50  
 51 Figure 2 – Overview of the transportation infrastructure monitoring strategy employing crowdsensing-based  
 52 techniques

53 It should be acknowledged that previous studies propose to use instrumented vehicles for transportation  
 54 infrastructure [9,10]. However, these instrumented vehicles are usually specially designed and are equipped

55 with expensive sensors, which means they cannot be used in a scalable manner due to the high cost [11]. This  
56 paper focuses on the utilization of commercial grade or naturally installed sensors in normal vehicles in order  
57 to gather data from a large number of vehicles for analysis. This type of monitoring technology offers several  
58 advantages: first, it can significantly reduce the cost for monitoring due to the voluntarily involvement of  
59 citizens; second, it has the potential to monitor a population of transportation infrastructure in real time; third,  
60 owing to big data, the technology is more robust to operational effects; fourth, the technology can be fully  
61 automated after the system is established.

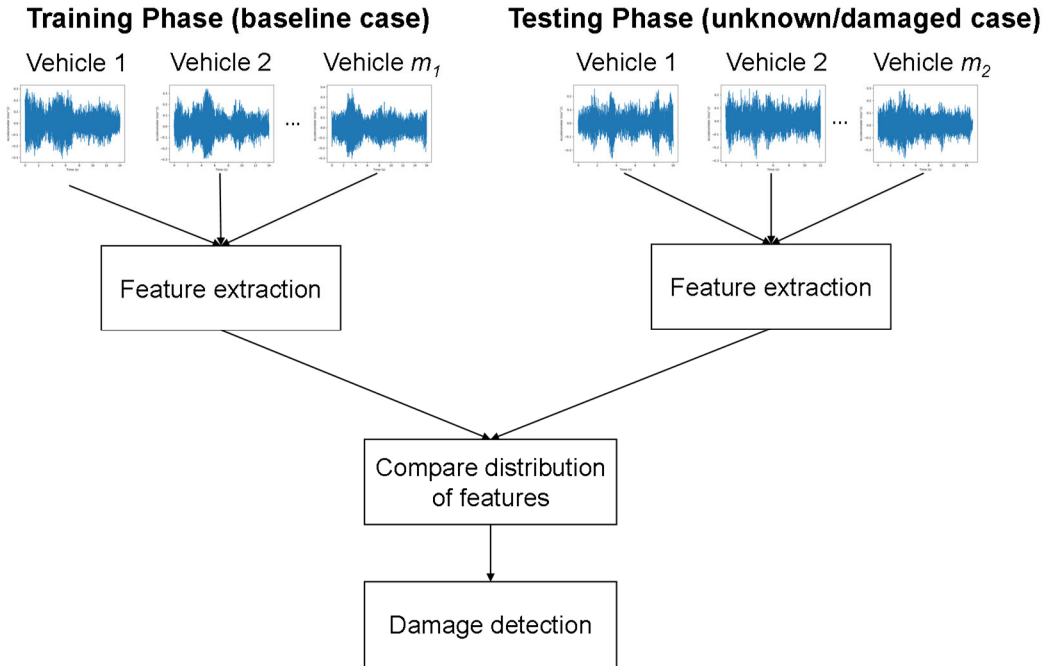
62 This paper will present three applications under the framework of crowdsensing-based transportation  
63 infrastructure monitoring using smartphones and sport cameras with which vehicles may be easily equipped.

## 64 **2. Application 1: Bridge Health Monitoring using Smartphones in Vehicles**

65 Moving sensors for bridge health monitoring have been investigated extensively in last decades [12-18].  
66 Yang et al. [14] were the first to conduct a study to extract the frequencies of a bridge from a moving vehicle.  
67 In their paper, the authors found an analytical solution showing that the data collected from a moving vehicle  
68 includes the dynamic properties of the bridge. Afterwards, numerical analysis and experiments were  
69 conducted by various researchers to show the feasibility of extracting dynamic properties such as frequencies,  
70 mode shape, or damping [13,18-21]. The major challenge in this research field is to separate the bridge  
71 properties from signals that mix bridge and vehicle vibrations. The mixed signals could also be affected by a  
72 number of factors such as road roughness and environmental effects.

73 Most of the previous studies focused on extracting the dynamic characteristics of the bridge using a  
74 single vehicle, which is sensitive to environmental and operational effects. In this paper, a new data-driven  
75 method for bridge damage detection based on a large number of vehicles is introduced. This method has the  
76 potential to be implemented on cars belonging to commuters, on police cars, on emergency vehicles, or on  
77 maintenance vehicles and buses to reduce costs associated with infrastructure monitoring.

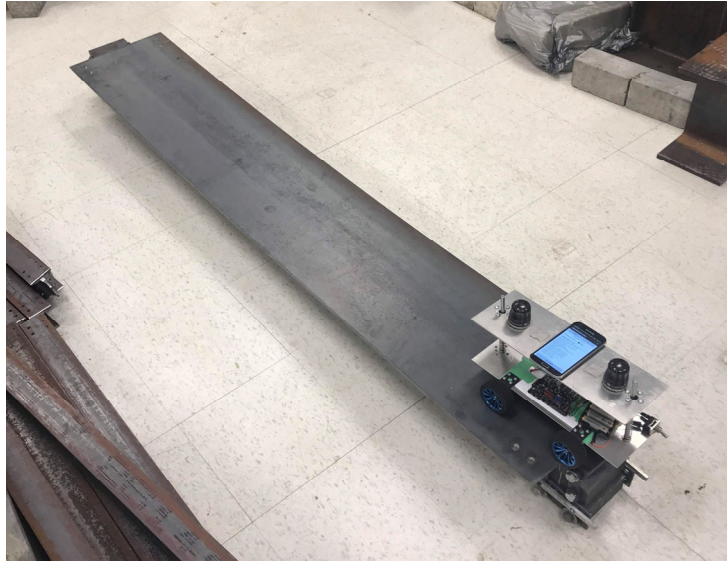
78 The overall method, shown in Figure 3, includes two phases; the training phase is the baseline case and  
79 the testing phase corresponds to the unknown state of the bridge. For each phase, acceleration data can be  
80 collected from a number of vehicles ( $m_1$  vehicles for training phase and  $m_2$  vehicles for testing phase).  
81 Features can be extracted from training and testing phases. The distribution of the features will then be  
82 compared to determine the existence of damage. The logic behind this method is that a large number of  
83 vehicles could mitigate the operational effects such as weight, suspension system, the speed of the vehicles,  
84 and the influence of other vehicles. Any large shift in terms of features should be observed only if the status  
85 of the bridge changes. In the research described in this paper, a Mel-frequency cepstral analysis is conducted  
86 for feature extraction, and Kullback–Leibler divergence is used for the comparison of feature distribution.  
87 Details of the method can be found in a previous study by the authors of the present work [6,22].



88  
89 Figure 3 – A crowdsensing-based bridge damage detection method

90 To verify the method described above, a lab experiment using smartphones in a robot car is conducted  
 91 as presented in Figure 4. In the experiment, a robot car passes through the bridge deck multiple times. The  
 92 robot car, as shown in Figure 5, is designed with the ability to change weight, spring constant, and speed to  
 93 mimic the behavior of vehicles of different configurations. The weight of the top plate could vary between  
 94 0.898, 0.988, 1.084, 1.170, and 1.270 kg; the spring constant could vary between 155, 288, 425, 615, and 726  
 95 N/m; and the speed of the robot car could be either 0.25, 0.33, or 0.40 m/s. Furthermore, each test is repeated  
 96 3 times to consider other effects such as road roughness. Two G-Link®-200 wireless accelerometers from  
 97 Microstrain Inc. and a Galaxy S5 smartphone from Samsung Group are mounted on the top plate of the robot  
 98 car. The sampling frequencies of the accelerometers and the smartphone are 128 Hz and 100 Hz, respectively.  
 99 An Android app was developed specifically for this purpose and installed on the smartphone to collect  
 100 vibration data. Details of the Android app can be found in a previous study by the authors of the present work  
 101 [6].

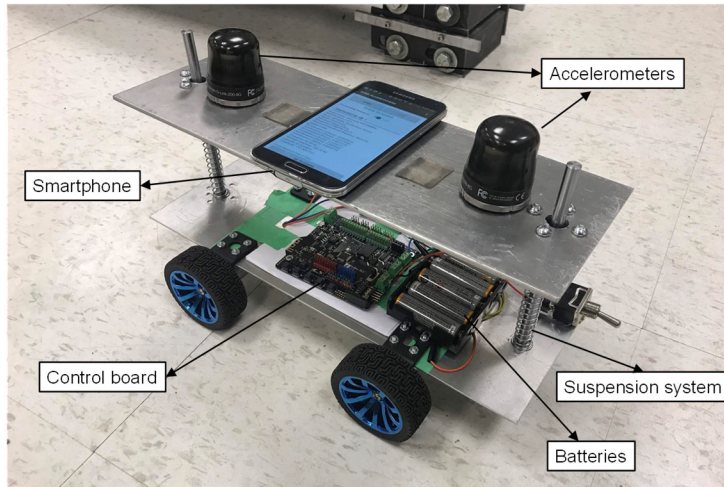
102 In total, three damage cases (DCs) are applied to the bridge: 1) 15% section area reduction at the mid-  
 103 span (see Figure 6); 2) 15% section area reduction at the  $\frac{1}{4}$  span (see Figure 6); and 3) boundary condition  
 104 changes at both ends, as shown in Figure 7(a) and (b). For each damage case, a total of  $5 \times 5 \times 3 \times 3 = 225$  tests  
 105 are completed considering the combination of all the possible robot car configurations and the repetition of  
 106 three times. In the analysis, 30 trials are conducted. In each trial, 50% of the 225 tests for each case are  
 107 randomly selected to simulate the randomness of the vehicle configurations.



108

109

Figure 4 – Lab experiment setup



110

111

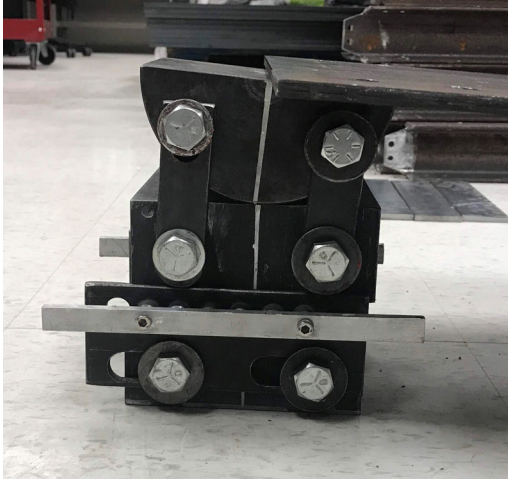
Figure 5 - Robot Car Configuration



112

113

Figure 6 – Local damage created by section area reduction



(a) Roller support



(b) Fixed support

Figure 7 – Global damage created by boundary condition changes

As shown in Eq. (1), damage feature is defined as a function of the Kullback–Leibler divergence.

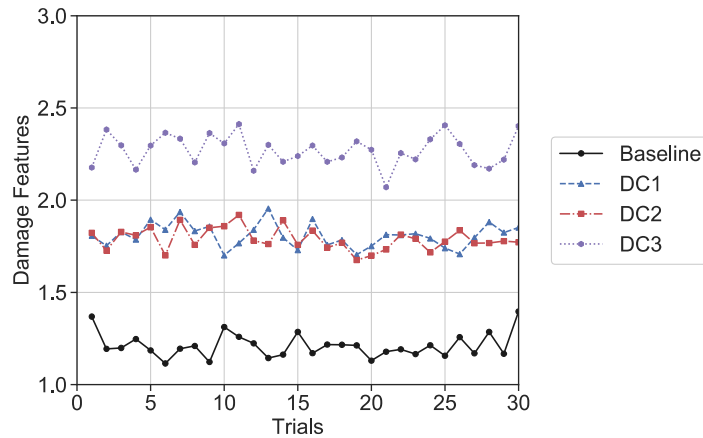
$$DF(F_{baseline}, F_{unknown}) = \ln(D_{KL}(F_{baseline}, F_{unknown}) + e) - 1 \quad (1)$$

where  $D_{KL}(F_{baseline}, F_{unknown})$  is the Kullback–Leibler divergence between the features of baseline and unknown cases, and  $e$  is the Euler's number. Assuming the features are Gaussian distributed, the Kullback–Leibler divergence can be calculated according to Eq. 2.

$$D_{KL}(F_{baseline}, F_{unknown}) = \frac{1}{2} \left[ \ln \frac{|\Sigma_{unknown}|}{|\Sigma_{baseline}|} + \text{trace}(\Sigma_{unknown}^{-1} \Sigma_{baseline}) + (\mu_{unknown} - \mu_{baseline})^T \Sigma_{unknown}^{-1} (\mu_{unknown} - \mu_{baseline}) - k \right] \quad (2)$$

where  $\mu_{baseline}$  and  $\mu_{unknown}$  are the average values of the features,  $\Sigma_{baseline}$  and  $\Sigma_{unknown}$  are the covariance matrices for baseline and unknown cases, and  $k$  is the number of features used for this analysis. In this study,  $k$  is set as 30. The function  $\text{trace}()$  calculates the trace of a matrix.

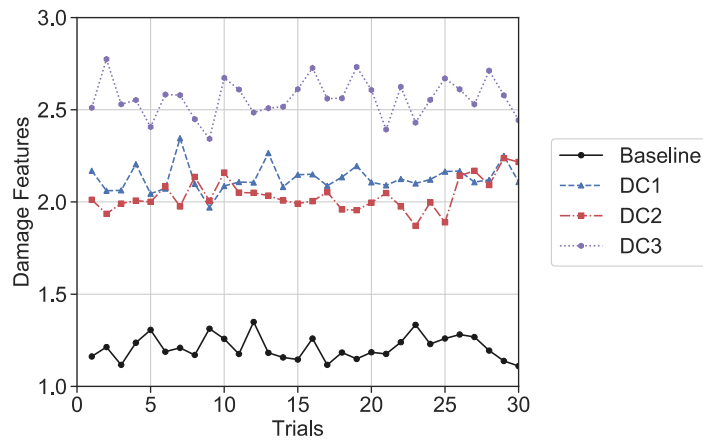
The damage features calculated using the data collected from the accelerometers and the smartphone are presented in Figure 8 and Figure 9. Each trial is related to a random sampling procedure of the vehicle configurations. As shown in the figures, the damage features are stable while different vehicles are used but the state of the bridge is unchanged. When the damage of the bridge is introduced (i.e., damage cases DC1, DC2, and DC3), the damage features become higher against the baseline case. This shows that the existence of damage is successfully identified. Comparing Figure 8 and Figure 9, we can see that the patterns of damage features from the accelerometers and the smartphone are very similar, which proves that the smartphone is suitable for this application even though it has lower resolution and sampling frequency.



130

131

Figure 8 – Damage features for baseline and three damage cases from the sensors



132

133

Figure 9 – Damage features for baseline and three damage cases from the smartphone

134

### 3. Application 2: Road inclination measurement using smartphones in vehicles

135

136

137

138

139

140

The gyroscope sensor can provide information regarding the orientation of the smartphone. In this section, a lab experiment investigating the feasibility of this sensor for road inclination measurement is introduced. As can be seen in Figure 10(a), 4 wooden decks are placed on the ground, and some small steel blocks are placed underneath these decks to create inclinations. The dimensions of the setup can be found in Figure 10(b). There are, in total, 4 zones in the setup, where zone 1 is flat, zone 2 is a decline with  $1.37^\circ$  inclination, zone 3 is an incline with  $0.96^\circ$  inclination, and zone 4 is a decline with  $1.37^\circ$  inclination.

141

142

143

144

145

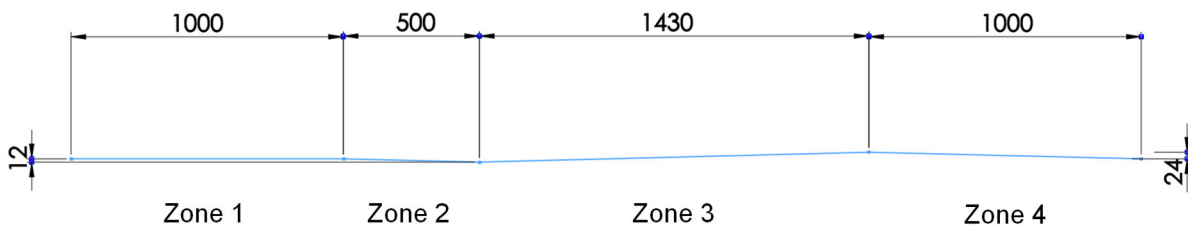
As shown in Figure 11(a) and (b), another version of the robot car similar to that used in the last section is used for this test. In this robot car, 4 rods instead of 2 rods are used for the stability of the top plate. The total weight of the top plate is 1.2 kg. One wireless accelerometer and one smartphone are placed on the top plate. It should be noted that data from the wireless accelerometer are not collected in this experiment. The Matlab app on the Android smartphone is used for this experiment.

146 The experiment includes three trials. As shown in Figure 12, the measured orientations are compared  
147 with the theoretical values (red dashed lines) calculated from the dimensions. As shown in the figure, the  
148 gyroscope sensor in the smartphone provides useful information about the deformation of the road. Some  
149 measurement errors exist, which could occur because the gyroscope sensor in the smartphone did not go  
150 through the calibration process before the tests. Also, the measurement is not accurate when the inclination  
151 of the decks changes because the robot car could cross over two decks at such locations. In a real-life scenario,  
152 the orientation information of the smartphones in multiple moving vehicles can be synchronized with the  
153 GPS data to show the deformation of the roads at city level. Challenges such as human factors should be  
154 resolved in real-life applications.



155  
156

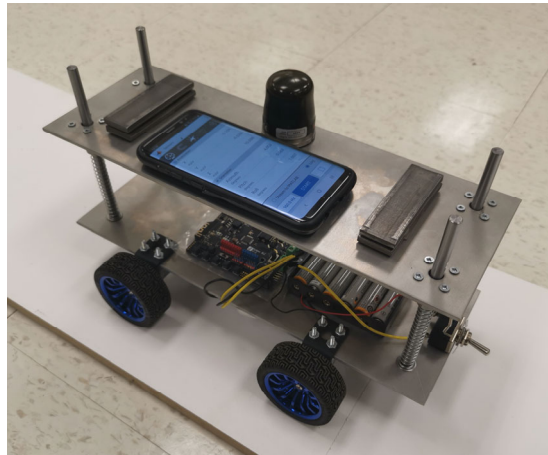
(a) Overview of the road deformation test setup



157  
158  
159

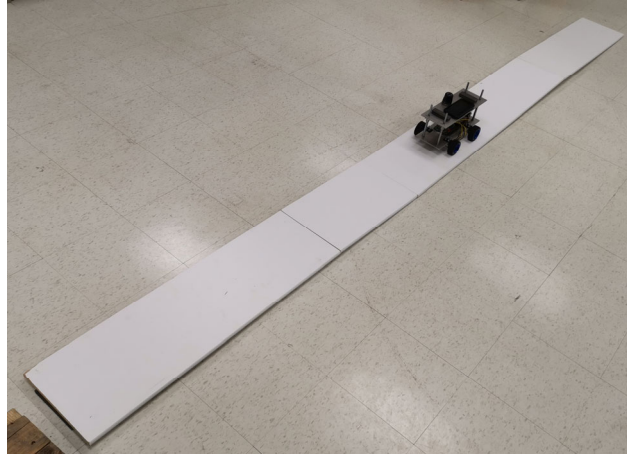
(b) Dimensions of the setup

Figure 10 - The deformed road setup and the dimensions (in mm)



160  
161

(a) Robot car for road deformation measurement



(b) Test procedure

Figure 11 – Road deformation measurement experiment

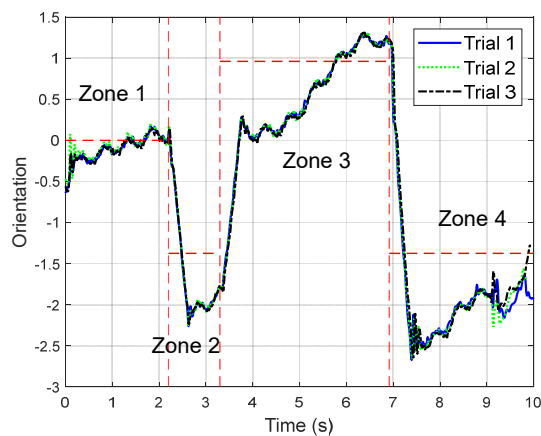


Figure 12 – Comparison of test results and theoretical values

162  
163  
164

165  
166

#### 167 **4. Application 3: Road crack detection using sport cameras attached to vehicles**

168 In addition to smartphones, backup cameras are another type of widely installed sensors in vehicles. In  
169 this section, the feasibility of applying such cameras for transportation infrastructure monitoring is  
170 investigated. Since current vehicles typically do not allow easy access to the backup camera system due to  
171 safety reasons, a commercial grade sport camera, GoPro, is mounted at the rear of the vehicle to mimic the  
172 behavior of a backup camera (see Figure 13). A sport camera can continuously capture videos at a high shutter  
173 speed.

174 In recent years, due to its ability to process massive data accurately and automatically, deep learning  
175 methods have attracted great attention of researchers in civil infrastructure monitoring [23]. They have been  
176 used to process vibration data [24-27] and image data [28-31] in different structures including bridges,  
177 buildings, railways and roads. For example, Rafiei and Adeli [24] designed a structural health index (SHI)  
178 based on synchrosqueezed wavelet transform, Fast Fourier Transform, and unsupervised deep Boltzmann  
179 machine. They used this index to assess the local and global condition of the structure. Dong et al. [32]  
180 proposed deep learning-based full field optical flow methods for structural displacement monitoring.

181 Particularly, deep learning-based methods have shown superior performance in the context of crack  
182 detection problems [33,29,34,35,28]. In this section, a novel deep learning algorithm is developed for road  
183 crack detection that considers the connectivity of pixels. The architecture of the deep neural network is  
184 presented in Figure 14. A batch size of 16 is used. Taking 256×256 color image patches extracted from GoPro  
185 as input, an encoder-decoder procedure is applied with multiple level feature fusion. The output of the deep  
186 neural network is a connectivity map, proposed in Mei et al. [36], representing the neighboring relationship  
187 of crack pixels. A depth-first search algorithm, as proposed in a previous study by the present authors [37],  
188 is applied to the output of the deep neural network to generate the binary mask for cracks. More details of the  
189 deep neural network can be found in the study authored by Mei et al. [36].

190 The deep neural network is first trained on a general image datasets ImageNet [38] as pre-training. Then,  
191 the proposed method is trained and tested on a dataset called EdmCrack600 released by our research team  
192 [39]. The EdmCrack600 dataset includes 600 images extracted from videos taken during approximately 10  
193 hours of driving in Edmonton, Canada. All the images were annotated manually at pixel level by the authors.  
194 The dataset was collected during road tests and consists of the various objects one can encounter during  
195 driving, such as snow, shadows from trees, other vehicles, etc.

196 In this study, the EdmCrack600 dataset is split into 420/60/120 images for training, validation, and  
197 testing purposes, respectively. After training for 20 epochs on EdmCrack600 dataset, the precision, recall,  
198 and F1 score, as defined in the work by Shi et al.[40], are calculated to measure the performance on the test  
199 set. The obtained precision, recall, and F1 score are 0.8469, 0.6994, and 0.7472, respectively. It took 251.09 s  
200 to process all 120 test images on a PC with Intel 8700k CPU, 32GB memory, and Nvidia Titan V GPU.  
201 Considering the memory limit of 11GB on GPU, the batch size of 16 is used, and overall implementation  
202 time includes the inference time from the deep neural network and the time for outputting the results The  
203 performance of this method on the EdmCrack600 dataset is comparable with the ones reported in a previous  
204 study by the present authors [41].



205  
206

Figure 13 – Mounting of GoPro Sport Camera

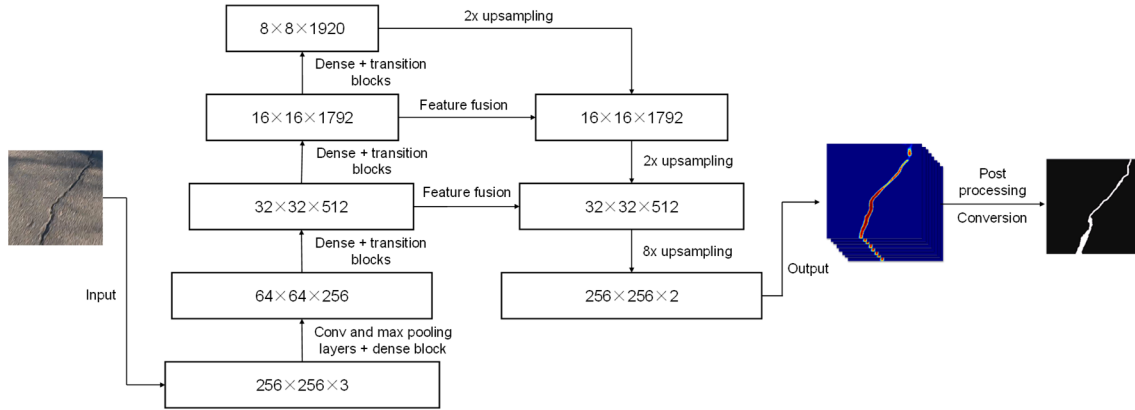
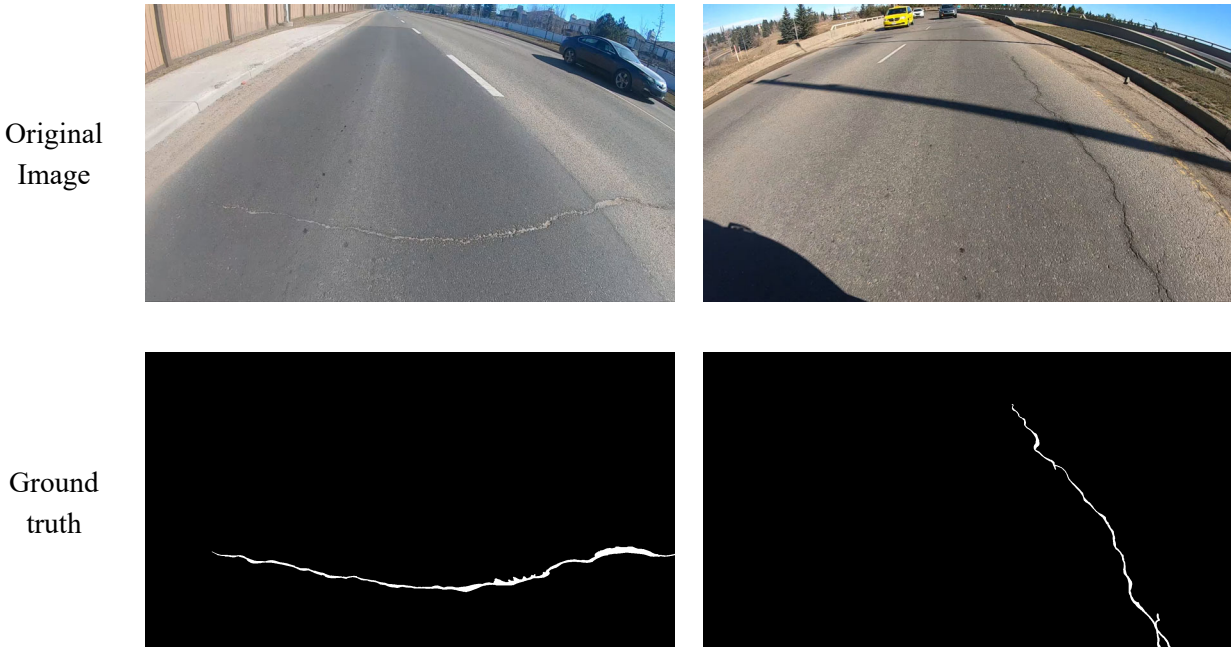
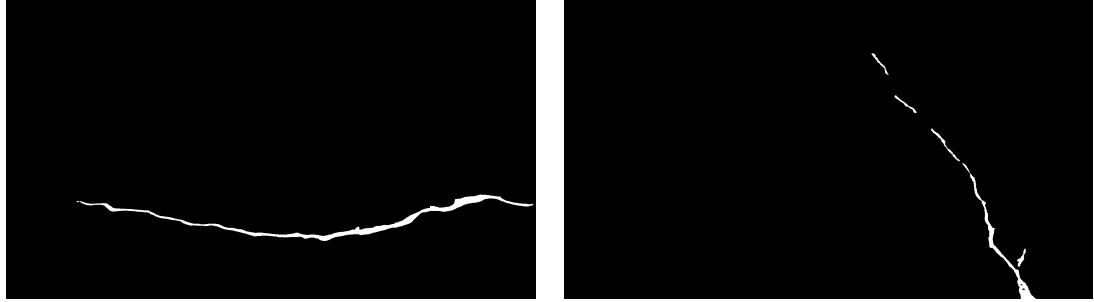


Figure 14 – Deep neural network architecture

Two sample images from the EdmCrack600 dataset and their corresponding identification results are shown in Figure 15. The images include many extraneous objects such as lane markers, shadows, and other vehicles which may affect the accuracy of crack detection. Comparing the ground truth and the identification results from our method, it can be seen that the cracks are correctly identified, and the influence of other objects is successfully excluded.



Our  
method



214 Figure 15 – Sample identification results from the deep learning-based method

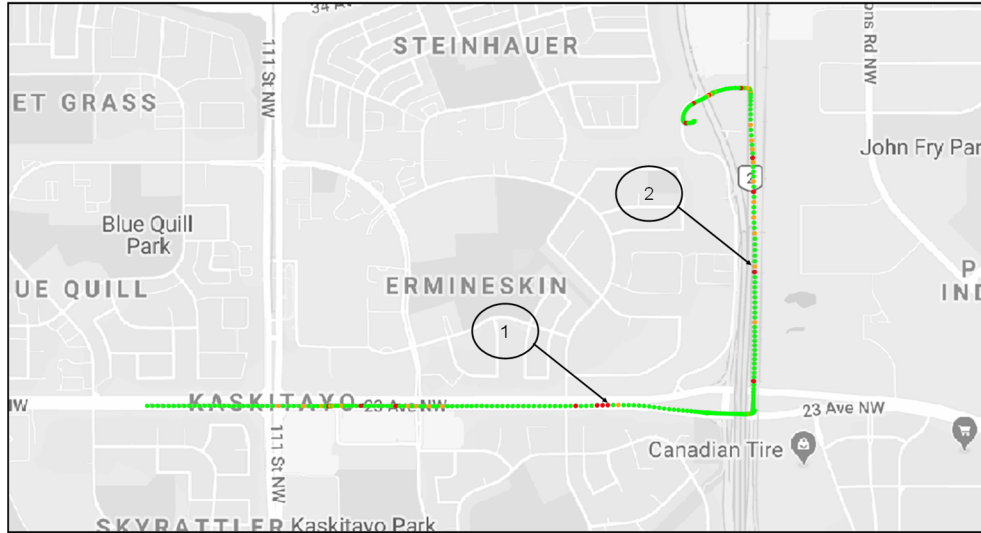
215 With the high success rate of road crack detection using our method, further analysis can be conducted  
216 by synthesizing the camera data with GPS signals collected by the GoPro. To quantitatively reflect the road  
217 condition, a simple crack index (CI) is designed as shown in Eq. 3.

$$CI = \frac{N_{crack}}{N_{total}} \times 1000 \quad (3)$$

218 where  $N_{crack}$  is the number of pixels that are identified as crack in an image and  $N_{total}$  is the total number of  
219 pixels in the image, i.e., resolution. A higher CI represents a worse road condition in terms of cracks.

220 Figure 16 is generated by calculating the CIs for a series of images taken at 0.5 s intervals over a time  
221 period of 410 s. The vehicle is driven such that it maintains the same speed as the surrounding traffic, and no  
222 extra effort is made to control the vehicle's speed. It should be noted that the images used herein were not  
223 annotated and not included in EdmCrack600 dataset. In the figure, each dot represents an image. The images  
224 with a CI smaller than 2 are colored green, the images with a crack index between 2 and 5 are yellow, and  
225 the others with a crack index higher than 5 are indicated in red. As shown in Figure 16, the road condition is  
226 worse in some locations than others.

227 Images at two locations, as labelled in Figure 16, and their corresponding results are presented in Figure  
228 17. The CIs for these two locations are 6.8 and 2.6, respectively. As illustrated in Figure 17, the cracks in the  
229 images are correctly identified, and the location 2 indeed has better road condition than location 1.

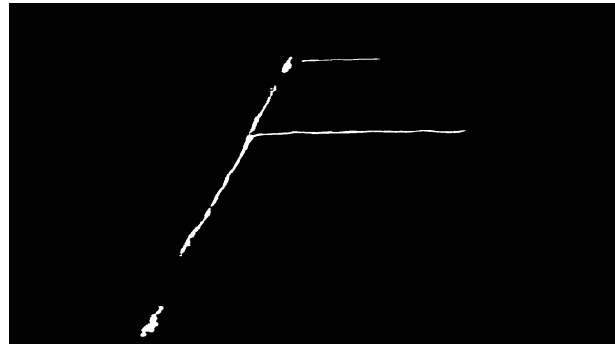


230  
231

Figure 16 – Crack index map calculated by synchronizing image and GPS data



(a) Original image at location 1



(b) Identification result at location 1



(c) Original image at location 2



(d) Identification result at location 2

232  
233

Figure 17 – Images and results from the two locations labelled in Figure 16

234 **5. Discussion**

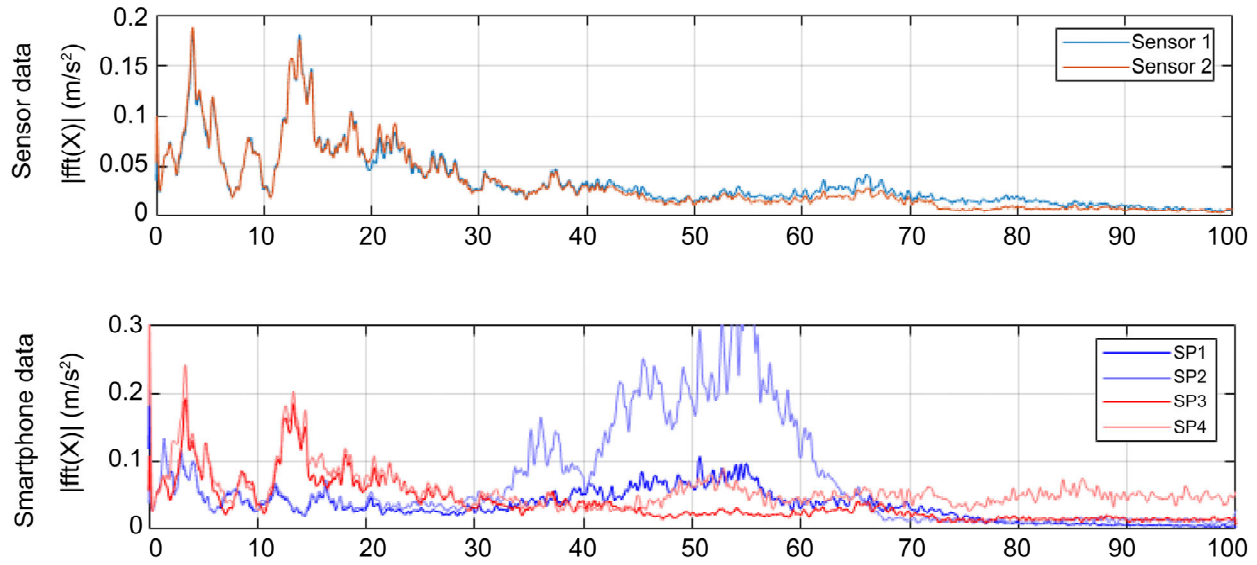
235 Although some experiments in the present study show the potential for the framework of crowdsensing-  
236 based transportation infrastructure monitoring , there are still many issues that need to be resolved before the  
237 framework can be applied to real-life monitoring. An important one is that the data collected from different  
238 vehicles using smartphones are influenced by vehicle and device properties. To investigate these effects,  
239 preliminary real-life data is collected from four bridges in Edmonton, i.e., Walterdale bridge, MacDonald  
240 bridge, Low Level bridge and High Level bridge. Two vehicles, one Honda Civic and one Honda Pilot, were  
241 used representing two vehicle types, sedan and SUV, respectively. In addition, in each vehicle two  
242 smartphones with sampling frequencies of 200 and 400 Hz are used, and two wireless accelerometers are  
243 used in the sedan as a benchmark to compare the performance of the smartphones.



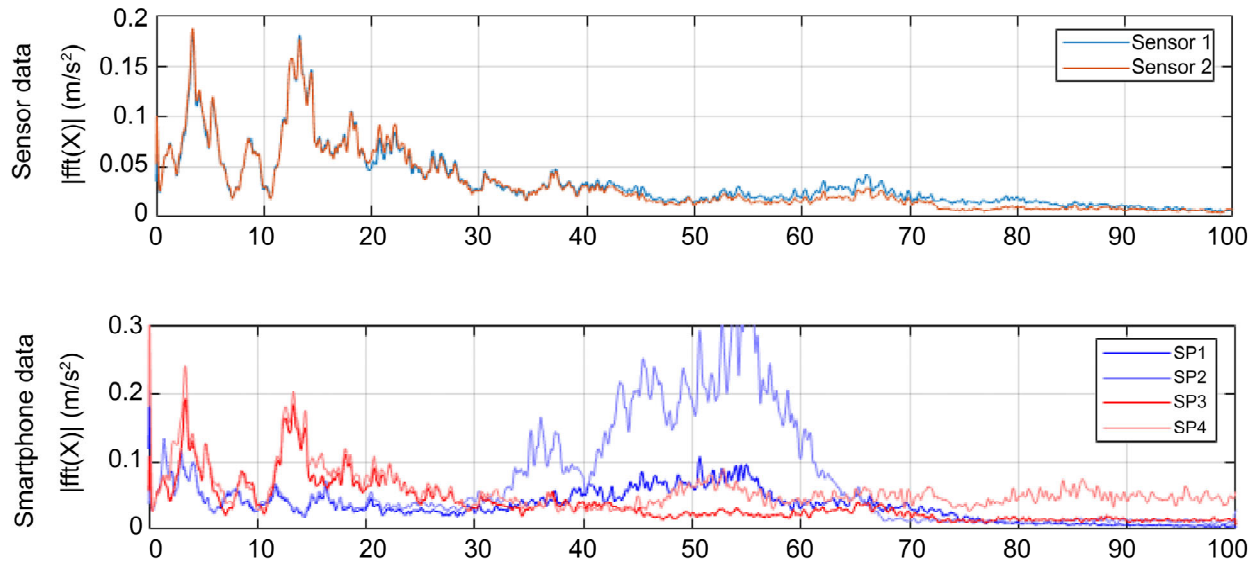
244  
245 Figure 18 – Image of the High Level bridge used for real-life study [42]

246 To present the results of the aforementioned investigation of the real-life issues due to the effects of  
247 vehicle and device properties, the frequency content of the data recorded on all devices while passing over

248 the High Level bridge (Figure 18) is illustrated in

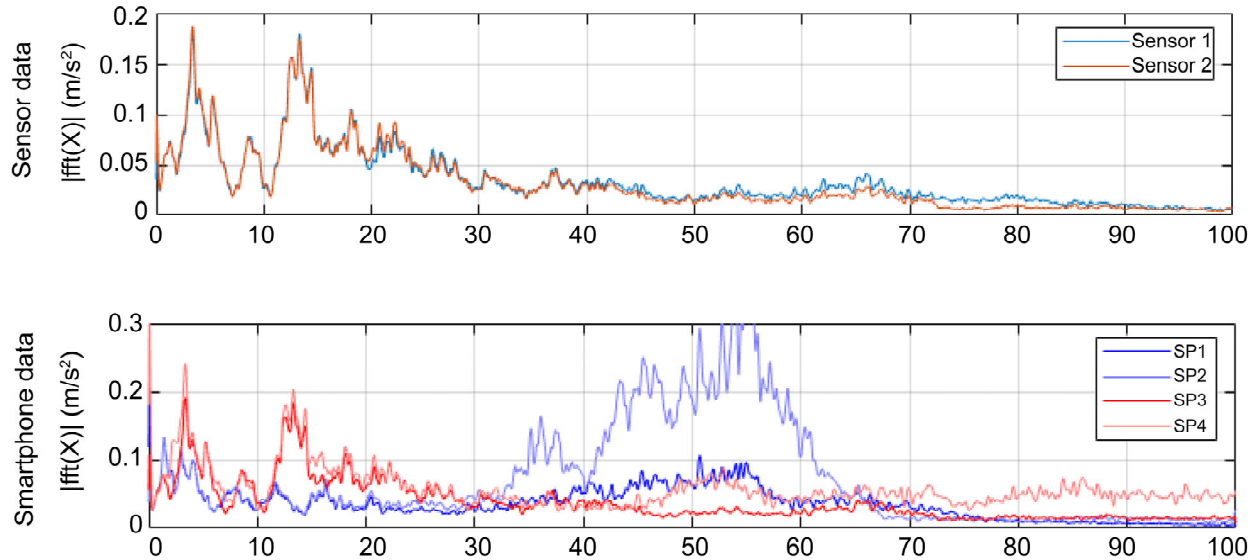


249  
250 Figure 19. The top and bottom plots show the sensor and smartphone data, respectively. The two sensors are  
251 installed on sedan, while the first two smartphones, denoted by SP1 and SP2, are installed in the SUV, and the  
252 other two smartphones, denoted by SP3 and SP4, are installed in the sedan. In addition, the sampling frequency  
253 of SP1 and SP3 is 200 Hz, while that of SP2 and SP4 is 400 Hz. As seen in



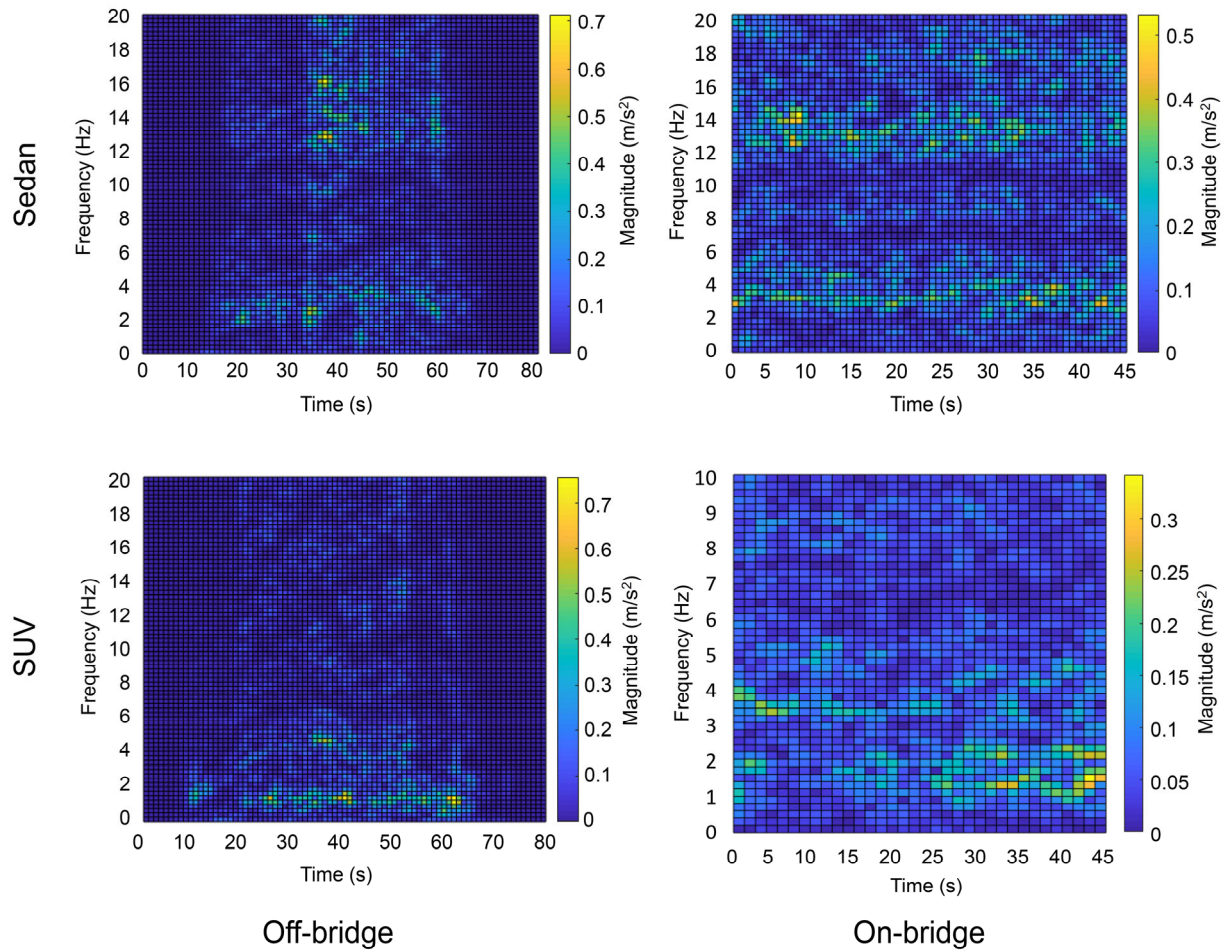
254  
255 Figure 19, the frequency content of the sensors and the smartphones located in the sedan, i.e., SP3 and  
256 SP4, follow similar patterns in the lower frequencies which proves the efficient performance of the  
257 smartphone in capturing major contents in lower frequencies, which are the focus for indirect bridge  
258 monitoring. Furthermore, comparing the smartphones with the 200 Hz sampling rate, i.e., SP1 and SP3, to  
259 the smartphones with the 400 Hz sampling rate, i.e. SP2 and SP4, shows similar agreement in lower  
260 frequencies, which eliminates the need to use higher sampling rates. On the other hand, comparing the data

261 from the SUV, i.e., SP1 and SP2, with the data from the sedan, i.e. SP3 and SP4, shows major differences,  
262 which indicates that the vehicle's features are the most significant factor affecting the frequency content of  
263 the acceleration signal recorded for the vehicle, and without considering this effect, it is difficult to employ  
264 indirect methods to capture frequency content of the bridge.



265  
266 Figure 19 – Frequency content of recorded acceleration signals while passing over the High Level bridge

267 To specifically study the effect of the vehicle, heat map plots of short time Fourier transform of each car  
268 while moving off-bridge and also while passing over the High Level bridge are illustrated in Figure 20. The  
269 off-bridge plots represent the condition in which the car is stopped, starts moving, and then stops, while the  
270 on-bridge plots are showing passing over the bridge with a constant speed. Comparing off-bridge and on-  
271 on-bridge plots corroborates the fact that the data collected from a vehicle passing over the bridge is significantly  
272 affected by the car type and features. In fact, these real-life data analyses prove that there is no general indirect  
273 monitoring method expected for extracting dynamic features of the bridge without considering the effect of  
274 the vehicle. One of the solutions to this issue is to create a filter to suppress car-related frequency content and  
275 hence amplify bridge-related content. Such a filter would need to be designed uniquely for each vehicle and  
276 cannot be generally used for any vehicle. Related work can be found in [43]. Another solution, as presented  
277 in section 2, could be to increase the number of the test vehicles in order to average out the effect of vehicles.



278  
 279 Figure 20 – Heat map of short time Fourier transform of recorded acceleration signals while moving off-bridge  
 280 and while passing over the High Level bridge

281 **6. Challenges**

282 Except the issues described in previous sections, there are many other challenges that have to be resolved  
 283 while building the crowdsensing based infrastructure monitoring system. One important challenge is the  
 284 influence of the vehicles themselves and of human beings on the collected data. The moving and vibration of  
 285 vehicles could corrupt the data like vibration data or images collected by the sensors. Also, devices in vehicles  
 286 could be moved and disturbed by the drivers or passengers during the data collection. Studies regarding these  
 287 effects should be taken. Advanced signal or image processing techniques would need to be applied to  
 288 eliminate the effects of the vehicles on the data.

289 Also, a trade-off must be made between the limited bandwidth available to transmit the raw data and the  
 290 large amount of computational power required to process the data. The onboard implementation of  
 291 computationally heavy algorithms, such as deep learning algorithms, to process the data is difficult, and the  
 292 computational capacity of vehicles and mobile devices is not as strong as that of remote servers. However,  
 293 the transmission of the raw data to remote servers for further analysis is limited by the bandwidth available.

294 In addition, since the moving vehicles are continuously collecting data while driving, it is challenging  
295 to attract a large number of users and keep them engaged in contributing to the monitoring purpose. Also,  
296 privacy issues should be addressed while collecting the data from the users. Relevant laws and regulations  
297 would need to be made regarding the disclosure of this type of data.

## 298 **7. Conclusions**

299 This paper proposes a framework for transportation infrastructure monitoring using moving vehicles.  
300 The feasibility of this framework and some relevant applications under this framework are investigated. This  
301 paper shows that the transportation infrastructure monitoring system established using crowdsourced moving  
302 vehicles is an automated prescreening tool which has the potential to monitor a large number of structures  
303 with reduced costs and increased efficiency compared with traditional civil infrastructure monitoring  
304 technologies.

305 Under this framework, three applications of smartphones and cameras for bridge and road health  
306 monitoring are presented. It is shown that it is feasible to use commercial-grade sensors equipped by smart  
307 devices in moving vehicles for preliminary transportation infrastructure monitoring. Further inspection could  
308 be only conducted on the structures with critical conditions. Specifically, the following conclusions can be  
309 drawn from this paper:

- 310 1) A methodology combining feature extraction and distribution comparison is proposed to take  
311 advantages of the vibration data from different vehicles at different times, which enables indirect  
312 bridge health monitoring from a large amount of data. Lab experiments are conducted to verify this  
313 method.
- 314 2) The gyroscope that can report the orientation of the smartphone is studied in this paper. The values  
315 reported by the gyroscope are compared with the actual inclinations in wooden decks in the lab  
316 experiment. The results show that the gyroscope in the smartphone has the potential to identify the  
317 large deformation in roads.
- 318 3) A deep learning algorithm combining connectivity maps and depth first search is proposed to  
319 identify cracks from moving vehicles. Testing on the EdmCrack600 dataset collected by our group,  
320 the proposed method can achieve the state-of-the-art performance. This algorithm enables efficient  
321 and cost-effective inspection of the road pavements. The image data are fused with GPS data in this  
322 study to provide the detailed information such as crack index of the pavement health condition in  
323 the neighborhood.

324 In the future, in the context of smart city, other sensors in smart devices and fusion of sensors will be  
325 investigated to provide more valuable information about current civil infrastructure systems.

## 326 **References**

- 327 1. Chourabi H, Nam T, Walker S, Gil-Garcia JR, Mellouli S, Nahon K, Pardo TA, Scholl HJ Understanding Smart  
328 Cities: An Integrative Framework. In: 2012 45th Hawaii International Conference on System Sciences, 4-7 Jan. 2012  
329 2012. pp 2289-2297. doi:10.1109/HICSS.2012.615

- 330 2. Gomes EH, Dantas MA, Macedo DDD, Rolt CRD, Dias J, Foschini L (2018) An infrastructure model for smart  
331 cities based on big data. *International Journal of Grid and Utility Computing* 9 (4):322-332
- 332 3. Angelidou M, Psaltoglou A, Komninou N, Kakderi C, Tsarchopoulos P, Panori A (2018) Enhancing sustainable  
333 urban development through smart city applications. *Journal of Science and Technology Policy Management* 9 (2):146-  
334 169
- 335 4. Engineers ASOC (2017) 2017 Infrastructure Report Card. [http://www.infrastructurereportcard.org/wp-](http://www.infrastructurereportcard.org/wp-content/uploads/2017/01/Bridges-Final.pdf)  
336 [content/uploads/2017/01/Bridges-Final.pdf](http://www.infrastructurereportcard.org/wp-content/uploads/2017/01/Bridges-Final.pdf).
- 337 5. Félío G (2016) Informing the Future: The Canadian Infrastructure Report Card.  
338 <http://canadianinfrastructure.ca/en/index.html>. Accessed October 18, 2019
- 339 6. Mei Q, Gül M (2018) A crowdsourcing-based methodology using smartphones for bridge health monitoring.  
340 *Structural Health Monitoring*:1475921718815457
- 341 7. Matarazzo TJ, Santi P, Pakzad SN, Carter K, Ratti C, Moaveni B, Osgood C, Jacob N (2018) Crowdsensing  
342 Framework for Monitoring Bridge Vibrations Using Moving Smartphones. *Proceedings of the IEEE* 106 (4):577-593.  
343 doi:10.1109/JPROC.2018.2808759
- 344 8. Metamorworks (2020). [https://www.shutterstock.com/zh/image-vector/autonomous-car-driving-on-road-](https://www.shutterstock.com/zh/image-vector/autonomous-car-driving-on-road-sensing-530358448?src=library)  
345 [sensing-530358448?src=library](https://www.shutterstock.com/zh/image-vector/autonomous-car-driving-on-road-sensing-530358448?src=library). Accessed January 25, 2020
- 346 9. Zalama E, Gómez-García-Bermejo J, Medina R, Llamas J (2014) Road crack detection using visual features  
347 extracted by Gabor filters. *Computer-Aided Civil and Infrastructure Engineering* 29 (5):342-358
- 348 10. Schnebele E, Tanyu B, Cervone G, Waters N (2015) Review of remote sensing methodologies for pavement  
349 management and assessment. *European Transport Research Review* 7 (2):7
- 350 11. Vavrik W, Evans L, Sargand S, Stefanski J (2013) PCR evaluation: considering transition from manual to semi-  
351 automated pavement distress collection and analysis.
- 352 12. Malekjafarian A, McGetrick PJ, OBrien EJ (2015) A review of indirect bridge monitoring using passing  
353 vehicles. *Shock and Vibration* 2015
- 354 13. OBrien EJ, Malekjafarian A (2016) A mode shape-based damage detection approach using laser measurement  
355 from a vehicle crossing a simply supported bridge. *Structural Control and Health Monitoring* 23 (10):1273-1286
- 356 14. Yang YB, Lin CW, Yau JD (2004) Extracting bridge frequencies from the dynamic response of a passing  
357 vehicle. *Journal of Sound and Vibration* 272 (3–5):471-493. doi:[http://dx.doi.org/10.1016/S0022-460X\(03\)00378-X](http://dx.doi.org/10.1016/S0022-460X(03)00378-X)
- 358 15. Matarazzo TJ, Pakzad SN (2018) Scalable structural modal identification using dynamic sensor network data  
359 with STRIDEX. *Computer-Aided Civil and Infrastructure Engineering* 33 (1):4-20
- 360 16. Matarazzo TJ, Pakzad SN (2016) Structural identification for mobile sensing with missing observations. *Journal*  
361 *of Engineering Mechanics* 142 (5):04016021
- 362 17. OBrien EJ, Malekjafarian A, González A (2017) Application of empirical mode decomposition to drive-by  
363 bridge damage detection. *European Journal of Mechanics-A/Solids* 61:151-163
- 364 18. Oshima Y, Yamamoto K, Sugiura K (2014) Damage assessment of a bridge based on mode shapes estimated  
365 by responses of passing vehicles. *Smart Structures and Systems* 13 (5):731-753
- 366 19. Keenahan J, OBrien EJ, McGetrick PJ, Gonzalez A (2014) The use of a dynamic truck–trailer drive-by system  
367 to monitor bridge damping. *Structural Health Monitoring* 13 (2):143-157. doi:10.1177/1475921713513974

- 368 20. Kim C-W, Isemoto R, Toshinami T, Kawatani M, McGetrick P, O'Brien EJ Experimental investigation of drive-  
369 by bridge inspection. In: 5th International Conference on Structural Health Monitoring of Intelligent Infrastructure  
370 (SHMII-5), Cancun, Mexico, 11-15 December, 2011, 2011. Instituto de Ingeniería, UNAM,
- 371 21. Shirzad-Ghaleroudkhani N, Mei Q, Gül M (2020) Frequency Identification of Bridges using Smartphones on  
372 Vehicles with Variable Features. *Journal of Bridge Engineering* 25 (7):04020041
- 373 22. Mei Q, Gül M, Boay M (2019) Indirect health monitoring of bridges using Mel-frequency cepstral coefficients  
374 and principal component analysis. *Mechanical Systems and Signal Processing* 119:523-546
- 375 23. Ye X, Jin T, Yun C (2019) A review on deep learning-based structural health monitoring of civil infrastructures.  
376 *Smart Structures and Systems* 24 (5):567-585
- 377 24. Rafiei MH, Adeli H (2018) A novel unsupervised deep learning model for global and local health condition  
378 assessment of structures. *Engineering Structures* 156:598-607
- 379 25. Li S, Zuo X, Li Z, Wang H (2020) Applying Deep Learning to Continuous Bridge Deflection Detected by Fiber  
380 Optic Gyroscope for Damage Detection. *Sensors* 20 (3):911
- 381 26. Khodabandehlou H, Pekcan G, Fadali MS (2019) Vibration-based structural condition assessment using  
382 convolution neural networks. *Structural Control and Health Monitoring* 26 (2):e2308
- 383 27. Zhang Y, Miyamori Y, Mikami S, Saito T (2019) Vibration-based structural state identification by a 1-  
384 dimensional convolutional neural network. *Computer-Aided Civil and Infrastructure Engineering* 34 (9):822-839
- 385 28. Dung CV, Anh LD (2019) Autonomous concrete crack detection using deep fully convolutional neural network.  
386 *Automation in Construction* 99:52-58. doi:<https://doi.org/10.1016/j.autcon.2018.11.028>
- 387 29. Liu Z, Cao Y, Wang Y, Wang W (2019) Computer vision-based concrete crack detection using U-net fully  
388 convolutional networks. *Automation in Construction* 104:129-139. doi:<https://doi.org/10.1016/j.autcon.2019.04.005>
- 389 30. Liu J, Yang X, Li L (2019) VibroNet: Recurrent neural networks with multi-target learning for image-based  
390 vibration frequency measurement. *Journal of Sound and Vibration* 457:51-66
- 391 31. Dhiman A, Klette R (2019) Pothole Detection Using Computer Vision and Learning. *IEEE Transactions on*  
392 *Intelligent Transportation Systems*
- 393 32. Dong C-Z, Celik O, Catbas FN, O'Brien EJ, Taylor S (2020) Structural displacement monitoring using deep  
394 learning-based full field optical flow methods. *Structure and Infrastructure Engineering* 16 (1):51-71
- 395 33. Cha YJ, Choi W, Büyüköztürk O (2017) Deep learning-based crack damage detection using convolutional  
396 neural networks. *Computer-Aided Civil and Infrastructure Engineering* 32 (5):361-378.  
397 doi:<https://doi.org/10.1111/mice.12263>
- 398 34. Yang F, Zhang L, Yu S, Prokhorov D, Mei X, Ling H (2019) Feature Pyramid and Hierarchical Boosting  
399 Network for Pavement Crack Detection. *IEEE Transactions on Intelligent Transportation Systems*.  
400 doi:<https://doi.org/10.1109/TITS.2019.2910595>
- 401 35. Zhang X, Rajan D, Story B (2019) Concrete crack detection using context-aware deep semantic segmentation  
402 network. *Computer-Aided Civil and Infrastructure Engineering*. doi:<http://dx.doi.org/10.1111/mice.12477>
- 403 36. Mei Q, Gül M, Azim MR (2020) Densely connected deep neural network considering connectivity of pixels  
404 for automatic crack detection. *Automation in Construction* 110:103018.  
405 doi:<https://doi.org/10.1016/j.autcon.2019.103018>

406 37. Mei Q, Gül M (2020) Multi-level feature fusion in densely connected deep-learning architecture and depth-first  
407 search for crack segmentation on images collected with smartphones. Structural Health Monitoring:1475921719896813

408 38. Deng J, Dong W, Socher R, Li L-J, Li K, Fei-Fei L Imagenet: A large-scale hierarchical image database. In:  
409 Computer Vision and Pattern Recognition, 2009. CVPR 2009. IEEE Conference on, 2009. Ieee, pp 248-255

410 39. Mei; Q, Gül; M (2019) EdmCrack600. <https://github.com/mqp2259/EdmCrack600>. Accessed July 10 2019

411 40. Shi Y, Cui L, Qi Z, Meng F, Chen Z (2016) Automatic road crack detection using random structured forests.  
412 IEEE Transactions on Intelligent Transportation Systems 17 (12):3434-3445.  
413 doi:<https://doi.org/10.1109/TITS.2016.2552248>

414 41. Mei Q, Gül M (2020) A cost effective solution for pavement crack inspection using cameras and deep neural  
415 networks. Construction and Building Materials 256:119397. doi:<https://doi.org/10.1016/j.conbuildmat.2020.119397>

416 42. Wikipedia (2020) High Level Bridge (Edmonton).  
417 [https://en.wikipedia.org/wiki/High\\_Level\\_Bridge\\_\(Edmonton\)](https://en.wikipedia.org/wiki/High_Level_Bridge_(Edmonton)). Accessed February 8, 2020

418 43. Shirzad-Ghaleroudkhani N, Gül M (2020) Inverse Filtering for Frequency Identification of Bridges Using  
419 Smartphones in Passing Vehicles: Fundamental Developments and Laboratory Verifications. Sensors 20 (4):1190

420

421

## List of Figures

- 422
- 423 Figure 1 – Sensors that can be installed in vehicles (modified from [8])
- 424 Figure 2 – Overview of the transportation infrastructure monitoring strategy employing crowdsensing-  
425 based techniques
- 426 Figure 3 – A crowdsensing-based bridge damage detection method
- 427 Figure 4 – Lab experiment setup
- 428 Figure 5 - Robot Car Configuration
- 429 Figure 6 – Local damage created by section area reduction
- 430 Figure 7 – Global damage created by boundary condition changes
- 431 Figure 8 – Damage features for baseline and three damage cases from the sensors
- 432 Figure 9 – Damage features for baseline and three damage cases from the smartphone
- 433 Figure 10 - The deformed road setup and the dimensions (in mm)
- 434 Figure 11 – Road deformation measurement experiment
- 435 Figure 12 – Comparison of test results and theoretical values
- 436 Figure 13 – Mounting of GoPro Sport Camera
- 437 Figure 14 – Deep neural network architecture
- 438 Figure 15 – Sample identification results from the deep learning-based method
- 439 Figure 16 – Crack index map calculated by synchronizing image and GPS data
- 440 Figure 17 – Images and results from the two locations labelled in Figure 16
- 441 Figure 18 – Image of the High Level bridge used for real-life study [42]
- 442 Figure 19 – Frequency content of recorded acceleration signals while passing over the High Level bridge
- 443 Figure 20 – Heat map of short time Fourier transform of recorded acceleration signals while moving  
444 off-bridge and while passing over the High Level bridge
- 445